Dedicated to Prof. Edith A. Turi in recognition of her leadership in education

COMONOMER DISTRIBUTION IN POLYETHYLENES ANALYSED BY DSC AFTER THERMAL FRACTIONATION

R. A. Shanks[*] and G. Amarasinghe

Department of Applied Chemistry, RMIT University, GPO Box 2476V, Melbourne, Victoria 3001
Australia

Abstract

Ethylene copolymers exhibit a broad range of comonomer distributions. Thermal fractionation was performed on different grades of copolymers in a differential scanning calorimeter (DSC). Subsequent melting scans of fractionated polyethylenes provided a series of endothermic peaks each corresponding to a particular branch density. The DSC melting peak temperature and the area under each fraction were used to determine the branch density for each melting peak in the thermal fractionated polyethylenes. High-density polyethylene (HDPE) showed no branches whereas linear low-density polyethylenes (LLDPE) exhibited a broad range of comonomer distributions. The distributions depended on the catalyst and comonomer type and whether the polymerisation was performed in the liquid or gas phase. The DSC curves contrast the very broad range of branching in Ziegler–Natta polymers, particularly those formed in the liquid phase, with those formed by single-site catalysts. The metallocene or single-site catalysed polymers showed, as expected, a narrower distribution of branching, but broader than sometimes described. The ultra low-density polyethylenes (ULDPE) can be regarded as partially melted at room temperature thus fractionation of ULDPE should continue to sub-ambient temperatures. The thermal fractionation is shown to be useful for determining the crystallisation behaviour of polyethylene blends.

Keywords: branch distribution, polyethylenes, single-site catalysts, thermal fractionation

Introduction

Linear low-density polyethylenes (LLDPE) are copolymers of ethylene and 1-olefins. They often exhibit multimodal branching distribution along the polymer chains. Due to the heterogeneity of the comonomer distribution, melting of LLDPEs continues over a broad temperature range, from above 50°C to just below 130°C, with the main melting peak at about 125°C. The differential scanning calorimetric (DSC) endotherms usually display one or two sharp peaks in the range of 120–125°C and a broad peak around 100–110°C covering the rest of the melting range [1, 2]. Therefore the crystal size or lamella thickness must consist of two or more overlapping distributions [3]. Mirabella [4] and Mathot [5] have detected the existence of re-

---
* Author for correspondence: e-mail: robert.shanks@rmit.edu.au

gions of different crystallinity in melt quenched LLDPEs. Moreover, it has been shown that LLDPEs undergo phase separation in the melt [4, 6] and evidence from small angle X-ray scattering of the melt has also suggested that LLDPE may have a two-phase liquid [7].

The branching distribution of LLDPEs has been quantitatively analysed using temperature rising elution fractionation (TREF) [8–17]. Two-dimensional fractionation by TREF and size exclusion chromatography (SEC) has shown that the distribution of branching is relatively independent of molar mass, except for very low molar mass fractions, which are highly branched [18]. In contrast, Hosoda [9] has found a trend towards less branching in the higher molar mass fractions. Nevertheless, the characterisation and branching distribution analysis of LLDPEs by various methods have recently been reported [19–38]. The most common methods are based on the subsequent analysis of melting behaviour of samples after applying a particular thermal treatment such as stepwise annealing [31], stepwise cooling [19–31], and successive self-nucleation/annealing (SSA) [32, 33] in a DSC. Moreover, the DSC fractionation method is considered to be quicker and an easier tool for analysing LLDPEs than TREF. In order to develop a faster method than TREF, Starck [29] has studied a series of commercial LLDPEs using stepwise crystallisation by DSC and compared the DSC data with those obtained by TREF. It has been found that the DSC technique is useful in characterising heterogeneity in comonomer distribution and providing relative analysis of comonomer distribution. Kamiya *et al.* [27] have performed a comparative study using a DSC fractionation technique based on stepwise crystallisation and TREF for a range of LLDPEs and made similar conclusions. Keating and co-workers have shown that DSC fractionation is a valuable tool in studying the structural effects such as crystallinity, molecular mass distribution, branch content, comonomer type and distribution of ethylene copolymers [21] and furthermore, elucidating the components of unidentified ethylene blends and tracking changes in grafting [23]. In addition, the DSC fractionation is found to be useful in studying phase separation behaviour of polymers [24].

Stepwise isothermal cooling of polyethylenes in a DSC has been shown to produce a series of melting peaks in a subsequent heating scan [19–31]. The series of melting peaks associates with a fractionation according to branch density and is called the melt memory effect [31] or thermal fractionation. The crystallisation at each isothermal step depends on the segment length between branches. Since TREF provides a separation of the polymer into individual fractions, only intermolecular fractionation is possible. On the other hand, in DSC, it is also possible for fractionation to occur intramolecularly. Thermal fractionation does not provide an extensive fractionation of the polymer into discrete phases; it must be thought of as an array of intermingled crystals with discrete lamella thicknesses. After heating to above the melting temperatures and then rapidly cooling, followed immediately by a second heating, all traces of the thermal fractionation are removed [31, 39]. Thermal fractionation has been applied to LLDPEs, often in conjunction with TREF [19, 20, 25, 26, 29]. The TREF results have been used to calibrate the thermal fractionation results since TREF provides fractions, which can be analysed independently by DSC,

FT-IR and NMR. Furthermore, an excellent correlation between TREF elution temperatures and DSC fractionation temperatures has been obtained by Zhang *et al*. [20].

Many new polyethylenes have been prepared and are now commercially available. The most prominent of these are being produced by metallocene or single-site catalysts. They provide a combination of more evenly spaced branches, increased branch content, narrow molar mass distribution and in some cases long chain branching. The densities for LLDPEs are normally around 0.920 g cm^{-3}. The polyethylenes, in which the densities are in between 0.89–0.91 g cm^{-3}, are called very low-density polyethylene (VLDPE) and those with densities less than 0.89 g cm^{-3}, are called ultra low-density polyethylene (ULDPE) [40].

Thermal fractionation can reveal the branching distribution in each of these new varieties of polyethylenes. The fractionation does not distinguish long branches. Short branches are excluded from the crystals, whereas the branch points of long branches are also excluded, however the long branches can participate in crystallisation. The amount of branches incorporated within the crystal greatly depends on the crystallisation conditions. It has been shown that rapid or quenched crystallisation can leave included branched points in the crystals [41]. The exclusion of branch points from crystals should be completed due to the long equilibration at each isothermal crystallisation temperature. Branches formed from the different comonomers, 1-butene (ethyl branch), 1-hexene (butyl branch), and 1-octene (hexyl branch) are excluded from crystals. Therefore, it is the presence of the branch point that is important, all of the short branches are not long enough to participate in crystallisation and so are excluded from the crystals. Conversely, other researchers have concluded that the branch length is not important, only the branch frequency, in determining crystallisation [42].

Low-density polyethylene (LDPE) can also be thermally fractionated to reveal its short chain branching distribution whereas high-density polyethylene (HDPE) shows no fractionation since it has no branches, or very few branches. In this research, we have used a DSC crystallisation method to fractionate various grades of polyethylenes. The branching distribution is then estimated by correlating fractionation data with the calibration curves derived from the literature. The results obtained for LLDPEs, VLDPEs and ULDPEs by this crystallisation method are presented and discussed in this paper.

Experimental

Materials

The polyethylenes used in this study are listed in Table 1. These polymers were chosen to represent LLDPEs with different types of 1-olefin comonomers, liquid and gas-phase polymerisation and various densities. 1-Butene, 1-hexene and 1-octene copolymers were supplied by Exxon Chemical, Orica Pty. Ltd. and Dow Plastics, Australia, respectively.

Table 1 Properties of polymers used in this study

Code	Comonomer	Catalyst type [a]	MFI/ g (10 min)$^{-1}$ [b]	Density/ g cm^{-3} [b]	T_{m^*}/ °C [c]	T_c/ °C [d]
HDPE	–	ZN	0.3	0.953	130	117
C$_4$-LLDPE1	butene	ZN	1.0	0.918	122	108
C$_4$-VLDPE1	butene	S	1.2	0.910	109	95
C$_4$-VLDPE2	butene	S	27.0	0.901	91	72
C$_4$-ULDPE1[e]	butene	S	3.0	0.878	63	52
C$_4$-LLDPE2	butene	ZN	1.0	0.912	123	104
C$_6$-LLDPE3	hexene	ZN	0.78	0.935	124	110
C$_8$-LLDPE4	octene	ZN	0.94	0.920	120	106
C$_8$-LLDPE5	octene	S	1.0	0.915	111	97
C$_8$-VLDPE3	octene	S	1.0	0.908	107	91
C$_8$-ULDPE2[e]	octene	S	0.5	0.870	60	47

[a]ZN=Ziegler–Natta catalyst, S=Single-site catalyst
[b]All data were taken from chemical data sheets published by the manufacture
[c]Crystallisation (T_c) and melting (T_{m^*}) temperatures were obtained at scanning rates of 10°C min^{-1}
[d]All cooling curves had a shoulder on the low-temperature side except for HDPE
[e]Very broad melting peaks were observed

Differential scanning calorimetry

A Perkin Elmer series Pyris1 differential scanning calorimeter (Pyris software version 3.0) was used for the thermal fractionation and thermal analyses. Samples (cut into thin slices), weighing about 2–5 mg, were sealed in crimped aluminium pans. The samples were heated under nitrogen and, the DSC was operated at ambient temperature mode with a cold finger cooled to 1–5°C with ice/water. Previous thermal effects were removed by melting the samples to 180°C and holding at 180°C for 5 min. The samples were then cooled to 25°C to obtain the crystallisation temperature (T_c) and heated again to 150°C to obtain the peak melting temperature (T_{m^*}). A cooling and heating rate of 10°C min^{-1} was used. A baseline was run with a similar empty pan using the same methods. The peak area and temperature calibrations were performed using pure indium.

Thermal fractionation method

After removing the previous thermal effects by holding the samples at 180°C for 5 min in the melt, the samples were cooled to 122°C at a nominal rate of 200°C min^{-1}. Isothermal crystallisation was continued for 50 min at 122°C. The sample was then cooled to 118°C at a 200°C min^{-1} rate and another isothermal crystallisation was followed. This procedure was repeated in every 4°C step until 46°C, then the samples were rapidly cooled to room temperature. For ULDPEs and C$_4$-VLDPE2, the samples were cooled to 98°C and isothermal crystallisation was repeated in every 4°C step un-

til 26°C. The melting scans were obtained by heating the thermal fractionated samples from 25 to 150°C at a 10°C min^{-1} heating rate.

Data analysis

The specific heat was calculated by using the multiple curve method on raw heat flow data. The degree of branching (B, branches per 1000 backbone carbon atoms) and degree of crystallinity (χ_c, %) were calculated from calibration curves derived from TREF results of previous researchers [9]. The relationships between peak melting temperatures (T_m), B and χ_c are as follows.

1-butene copolymers	$T_m = -1.55B+134,$	$\chi_c = -1.32B+82$
1-hexene comonomers	$T_m = -1.69B+133,$	$\chi_c = -1.34B+77$
1-octene comonomers	$T_m = -2.18B+134,$	$\chi_c = -2.51B+86$

The amount of polymer in each fraction (Table 2) was then estimated using the calculated crystallinity values and area under each endotherm (A); % Polymer= (A/%χ_c)×100.

Results and discussion

Distinction between liquid and gas phase LLDPE

Figure 1 shows the DSC curve for a gas phase polymerised C$_6$-LLDPE3 after thermal fractionation. The stepwise cooling program caused a series of 11 melting peaks in the range of 81–135°C and their separation. The peaks also enhanced the view of the distribution of branches that can be otherwise seen from the broad melting endotherm observed in melting after continuously cooling of the LLDPE (shown as a dotted line). Liquid phase Ziegler–Natta catalysed C$_8$-LLDPE4 (Fig. 2) displayed 10 peaks between 84 and 131°C and showed the presence of a greater proportion of more highly branched molecules. It can also be seen from Figs 1 and 2 that the more branched segments in C$_8$-LLDPE4 are much more prevalent than in the gas phase C$_6$-LLDPE3. The sharp peak at 125°C is relatively smaller than that of the gas phase LLDPE with the same comonomer composition (~5 mol%). The peaks in the range of
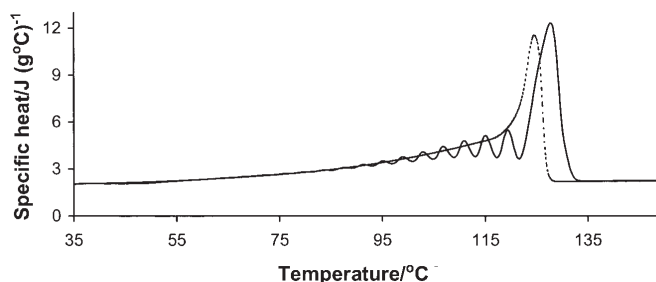
Fig. 1 DSC specific heat curves of gas phase polymerised C$_6$-LLDPE3. — after thermal fractionation and ---- after cooling at a rate of 10°C min^{-1}

100–120°C are larger. This may reflect a difference in the nature of the catalyst in each system or, in part, extractions of some of the more highly branched molecules by the hydrocarbon solvent in the liquid phase system. Liquid phase LLDPEs have been found to have a lower level of hexane extractables. Another difference in the LLDPEs is that the liquid phase polymer is an octene copolymer, while the gas phase polymer is a hexene copolymer. Balbontin *et al.* have also found that LLDPEs show very distinct comonomer distributions depending on the catalyst type [26].

Calibration curves based on published results for TREF [9] with the DSC melting temperature of each fraction were used to determine the branch density for each melting peak in the thermal fractionated polyethylenes. The amount of each branch density was calculated from the area under each peak after correction for the crystallinity of a polyethylene with that branch density. This provided a complete analysis of the branch distribution in the polyethylenes. Results obtained for the three
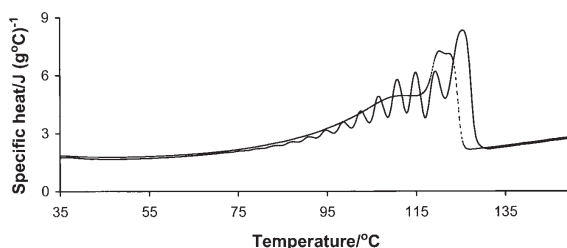
Fig. 2 DSC specific heat curves of liquid phase polymerised C_8-LLDPE4. — after thermal fractionation and ---- after cooling at a rate of 10°C min^{-1}
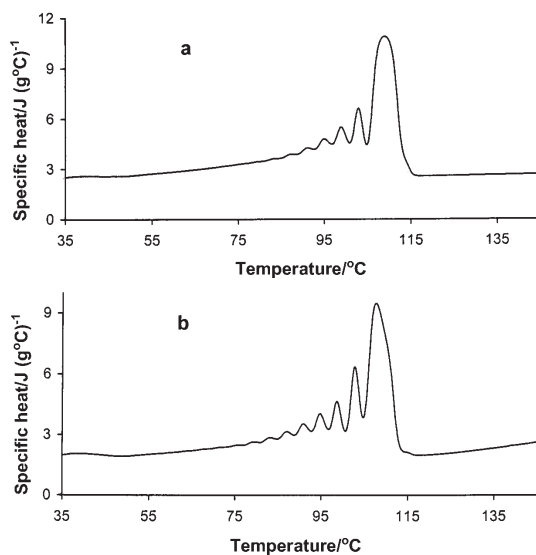
Fig. 3 DSC specific heat curves of a) C_4-VLDPE1, D=0.910 g cm^{-3} and b) C_8-LLDPE5, D=0.908 g cm^{-3} after thermal fractionation

LLDPEs are given in Table 2. This method has also been used to provide similar data for each of the polyethylene examples shown in this paper.

The DSC curves of two thermally fractionated VLDPEs with similar densities are shown in Figs 3a and 3b. Metallocene-catalysed C_4-VLDPE1 gave 6 peaks between 85–118°C, whereas C_8-VLDPE3, made with non-metallocene single-site catalyst [43], exhibited 9 peaks with the lowest and highest peak melting temperatures appearing at 76 and 107°C. These results indicate that there is a distribution of branching but that there are no molecules or segments with few branches as in LLDPEs. However, these VLDPEs are expected to have more uniform and narrower branching distribution due to the single active site of the catalyst used. Such structural heterogeneity of metallocene-made polymers has also been reported by Hsieh *et al.* [16].

Figure 4A presents the DSC melting curves for thermally fractionated polymers, which are ordered according to the decreased densities. It can be seen that the melting temperatures decrease as the densities decrease. The set of DSC curves enabled clear comparison of each of the branching densities present. The peak melting temperatures for all polymers were the same since they were determined by the stepwise isothermal temperatures used in the thermal fractionation (Table 2). The DSC curve of HDPE (Fig. 4a) was included for comparison and to demonstrate that no thermal fractionation was observed since there was no branching present. The C_4-LLDPE1 is also a gas-phase Ziegler–Natta catalysed polymer and, the DSC curve (Fig. 4b) exhibits a
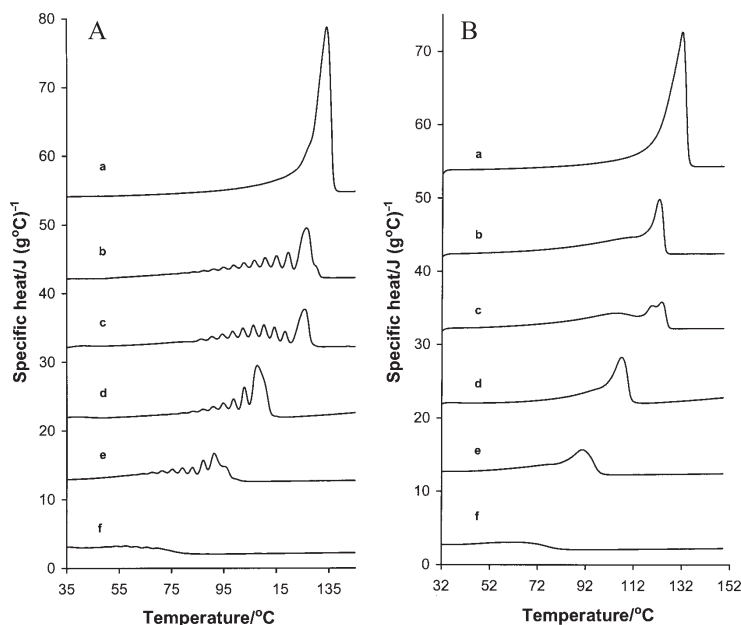
Fig. 4 DSC specific heat curves of polymers after A) thermal fractionation and B) after cooling at a rate of 10°C min^{-1}. a) HDPE, b) C_4-LLDPE1, c) C_4-LLDPE2, d) C_8-VLDPE3, e) C_4-VLDPE2 and f) C_4-ULDPE1. An adapted scale is drawn by consecutively adding 10 units to each curve

similar pattern to that of C_6-LLDPE3 (Fig. 1). However, it is interesting to note that C_4-LLDPE2 (Fig. 4c), which is a Ziegler–Natta catalysed polymer [44] shows a much greater proportion of more highly branched molecules in the range of 90–100°C as seen in the C_8-LLDPE4. Single-site catalysed C_8-VLDPE3 and C_4-ULDPE1 (Figs 4e and 4f) demonstrated series of peaks indicating the existence of much broader distribution of branching.

The DSC curves for the same polymers after continuous cooling in the DSC at 10°C min^{-1} from 180 to 25°C are shown in Fig. 4B. These normal DSC curves did not convey the more detailed information available from the thermally fractionated samples, other than to assume that copolymers with multiple peaked DSC curves have substantial crystallite heterogeneity. They were essentially the same as a smoothed version of the thermally fractionated samples except they were shifted to lower melting temperatures since crystallisation was performed more rapidly. Crystallisation (T_c) and melting temperatures (T_{m*}) of polymers obtained at scanning rates of 10°C min^{-1} are given in Table 1.

Table 2 Branching distribution and proportion of polymer in each fraction of LLDPEs

T_m/ °C [a]	C$_4$- LLDPE1		C$_6$-LLDPE2		C$_8$-LLDPE3	
	Branching[b]	%Polymer	Branching[b]	%Polymer	Branching[b]	%Polymer
125	5	28.9	3	40.1	4	23.2
119	9	9.0	8	7.9	7	11.9
115	12	8.5	11	7.6	9	11.1
111	15	8.8	13	7.4	11	11.7
107	18	8.0	15	6.7	13	10.2
103	20	7.4	18	6.3	14	8.8
99	23	7.0	20	5.7	16	6.9
95	25	6.2	22	5.2	18	6.4
91	28	5.9	24	4.6	20	5.3
87	30	5.3	27	4.4	21	4.5
83	33	4.9	29	4.0		

[a]Peak melting temperature of each fraction; [b]Branches per 1000°C.

The DSC heating curves for ULDPEs after thermal fractionation are illustrated in Fig. 5. These polyethylenes are often called polyethylene elastomers. The melting process of ULDPEs extended across a large temperature range (25–85°C) immediately starting at room temperature. Furthermore, it was noted that the fractionated samples of ULDPEs analysed after a week had lost their fractionation upon storage at room temperature. Thus, ULDPEs can be regarded as polyethylenes, which are partially melted at room temperature and the pellets have a tendency to clump together upon storage. Crystallisation at a temperature below room temperature, such as down to –60°C, can allow further crystallisation. After such low temperature of crystallisation, the ULDPE can be analysed from as low as –60°C. This means that segments
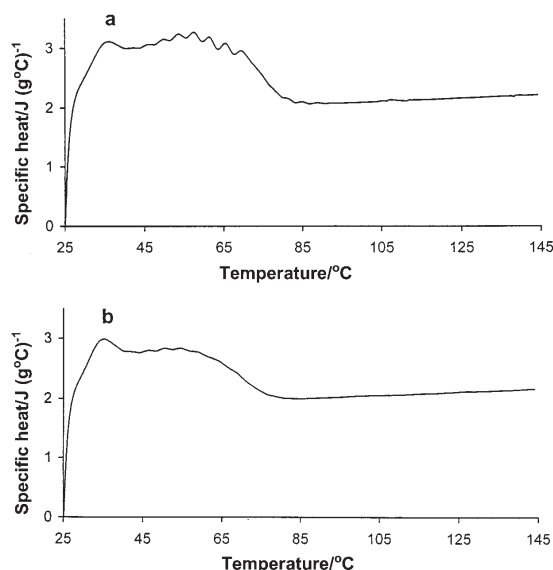
Fig. 5 DSC specific heat curves of a) C_4-ULDPE1 and b) C_8-ULDPE2 after thermal fractionation

with short lengths between branches are able to crystallise and form very thin lamella. It has been reported the poly(ethylene-co-propylene) elastomers can crystallise if they are held at sub-ambient temperatures (–60°C) and then heated to analyse the melting characteristics [2].

The low melting temperatures of ULDPEs causes a problem with the baseline since melting starts immediately upon heating in the DSC. When converting the results to a specific heat curve an isothermal period at the start of the scan is required for comparison with a separately recorded empty pan baseline. It is often not possible to have a stable or correct isothermal period because the sample is not at equilibrium. This results in values of the specific heat different from the values of about 2 J g^{-1} °C^{-1} which are typical of polyethylenes.

If it is assumed that there is an equilibrium melting temperature (T_m°) for polyethylenes. This will be the maximum lamella thickness for the chain folded crystalline form. The lamella thickness can be calculated for each of the peak temperatures formed by the thermal fractionation. This provides an estimate of the lamella thicknesses associated with the low melting crystals, including those that melt below room temperature. There is a problem with these calculations in that polyethylenes often rearrange on heating during the DSC scan and so the Gibbs-Thompson equation must be used with caution [45]. In the case of thermally fractionated polyethylenes rearrangement is minimal because the samples have been stepwise crystallised over a period of 12–15 h so they are close to equilibrium. Under normal cooling conditions such as 10°C min^{-1} in the DSC we have observed considerable rearrangement on melting. This takes the form of double melting endotherms instead of the sharper highest melting peak in LLDPE. Often the re-

arranged melting peak is the predominant peak. Figures 1 and 2 demonstrated the higher melting temperatures obtained after thermal fractionation compared with cooling at $10°C\ min^{-1}$.

Thermal fractionation is particularly useful for characterising blends of polyethylenes [21, 46–48]. Figure 6 presents the DSC specific heat curves for the blends of C_8-LLDPE4 and C_8-LLDPE5 and pure component polymers after thermal fractionation. The curves for the blends can be seen to be the sum of the two components. If the component specific heat curves were added in the proportion that they were present in the blend then a calculated DSC specific heat curves for the blend was obtained. Comparison of the calculated and measured blends showed the degree of additivity of the blend. The overlaid thin solid lines represent the calculated curves for the 20% and 80% C_8-LLDPE5 blends. The calculated and observed curves were closely matched in the 20% blend indicating that two polymers could have crystallised independently. On the other hand, 80% blend displayed significant differences between the calculated and observed curves. The calculated curve of 80% C_8-LLDPE5 showed a single broad peak for the main melting peak of C_8-LLDPE5, whereas the observed curve contained two resolved peaks for the same temperature range. This suggested that polymers were having an effect on their crystallisation in the blend. Therefore, it is apparent that two polymers in the 80% blend may be miscible or partially miscible and are able to co-crystallise. If the two polymers are miscible in the liquid, then when segments crystallise they do so with segments of
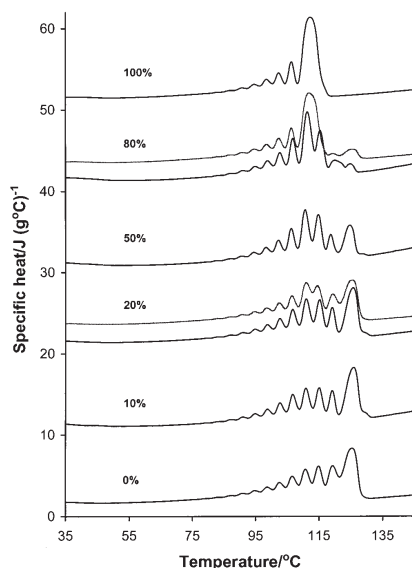
Fig. 6 DSC specific heat curves of C_8-LLDPE4 and C_8-LLDPE5 blends after thermal fractionation. The percentage figure refers to the percentage of C_8-LLDPE5 in the blend. Thin solid lines represent the calculated specific heat curves for the 20 and 80% C_8-LLDPE5 blends. An adapted scale is drawn by consecutively adding 10 units to each experimental curve and 12 units to each calculated curve

similar length between branches, so the two polymers are able to co-crystallise where they have common segment lengths. Similar analysis has been carried out by Arnal *et al*. [47, 48] on HDPE-LLDPE blends after the SSA thermal treatment. The partial miscibility of HDPE-LLDPE blends is also evident by the co-crystallisation of linear fractions.

Conclusions

All ethylene copolymers studied exhibit a wide range of comonomer distributions. The distributions depend on the catalyst and comonomer type and whether the polymerisation is in liquid or gas phase. The Ziegler–Natta polymers show a very broad range of branching, particularly in those formed in the liquid phase compared with those formed in the gas phase. The metallocene or single-site catalysed polymers show, as expected, a narrow distribution of branching, but much broader than often described. Since ULDPEs are partially melted at room temperature, it is necessary to choose subambient temperatures for the complete evaluation. The observation for HDPE confirms that the thermal fractionation phenomenon is caused by branch distribution, not molar mass distribution. Thermal fractionation is also useful in characterising polyethylene blends. Added specific heat curves suggest that higher C_8-LLDPE5 blends may be miscible and able to co-crystallise, whereas lower blends are thought not be miscible.

<p style="text-align:center">* * *</p>

References

 1 A. Prasad, Polym. Eng. & Sci., 38 (1998) 1716.

 2 V. B. F. Mathot, Calorimetry and Thermal Analysis of Polymers, Hanser: New York 1993, Chapter 9, p. 232.

 3 V. B. F. Mathot, R. L. Scherrenberg and T. F. J. Pijpers, Polymer, 39 (1998) 4541.

 4 F. M. Mirabella, S. P. Westphal, P. L. Fernando, E. A. Ford and J. G. Williams, J. Polym. Sci., Polym. Phys. Ed., 26B (1988) 1995.

 5 R. A. C. Debilieck and M. B. F. Mathot, J. Mat. Sci. Lett., 7 (1988) 1276.

 6 a) M. J. Hill and P. J. Barham, Polymer, 35 (1994) 1802. b) R. Morgan, M. J. Hill, P. J. Barham and C. Frye, Polymer, 38 (1997) 1903.

 7 I. G. Voight-Martin, R. G. Alamo and L. Mandelkern, J. Polym. Sci., Polym. Phys. Ed., 24 (1986) 1283.

 8 L. Wild, Adv. Polym. Sci., 98 (1991) 1 and references therein.

 9 S. Hosoda, Polym. J., 20 (1988) 383.

10 C. J. Neves, E. Monteiro and A. C. Habert, J. Appl. Polym. Sci., 50 (1995) 817.

11 F. Defoor, G. Groeninckx, H. Reynaers, P. Schouterden and B. Van der Heijden, J. Appl. Polym. Sci., 47 (1993) 1839.

12 A. Barbalata, T. Bohossian and G. Delmas, J. Appl. Polym. Sci., 46 (1992) 411.

13 E. Karbashewski, L. Kale, A. Rudin, W. J. Tchir, D. G. Cook and J. O. Pronovost, J. Appl. Polym. Sci., 44 (1992) 425.

14 P. L. Joskowicz, A. Muñoz, J. Barrera and A. Müller, Macromol. Chem. Phys., 196 (1995) 385.

15 X. Zhou and J. N. Hay, Eur. Polym. J., 29 (1993) 291.

16 E. T. Hsieh, C. C. Tso, J. D. Byers, T. W. Johnson, Q. Fu and S. Z. D. Cheng, J. Macromol. Sci.-Phys., B36 (1997) 615.

17 Y. Feng and X. Jin, Polym. Plast. Tech. Eng., 37 (1998) 271.

18 V. B. F. Mathot, Calorimetry and Thermal Analysis of Polymers, Hanser: New York 1993, Chapter 9, p. 286.

19 E. Adisson, M. Ribeiro, A. Deffieux and M. Fontanille, Polymer, 33 (1992) 4337.

20 M. Zhang, J. Huang, D. Lynch and S. E. Wanke, ANTEC Proceed., (1998) 539.

21 M. Y. Keating and E. F. McCord, Thermochim. Acta, 243 (1994) 129.

22 F. C. Chiu, M. Y. Keating and S. Z. D. Cheng, ANTEC Proceed., (1995) 1503.

23 M. Y. Keating, I. –H. Lee and C. S. Wong, Thermochim. Acta, 284 (1996) 47.

24 Q. Fu, F. C. Chiu, K. W. McCreight, M. Guo, W. W. Tseng, S. Z. D. Cheng, M. Y. Keating, E. T. Heish and P. DesLauriers, J. Macromol. Sci., Phys., B36 (1997) 41.

25 G. Balbontin, L. Camurati, T. Dall'Occo, A. Finotti, R. Franzese and G. Vecellio, Angew. Makromol. Chemie, 219 (1994) 139.

26 G. Balbontin, L. Camurati, T. Dall'Occo and R. Zeigler, J. Mol. Catalyst A: Chemical, 98 (1995) 123.

27 T. Kamiya, N. Ishikawa, S. Kambe, N. Ikegami, H. Nishibu and T. Hattori, ANTEC Proceed., (1990) 871.

28 R. A. Shanks and K. M. Drummond, ANTEC Proceed., (1998) 2004.

29 P. Starck, Polym. Intern., 40 (1996) 111.

30 B. Wolf, S. Kenig, J. Klopstock and J. Miltz, J. Appl. Polym. Sci., 62 (1996) 1339.

31 J. Varga, J. Menczel and A. Solti, J. Thermal Anal., 17 (1979) 333.

32 A. J. Müller, Z. H. Heránndez, M. L. Arnal and J. J. Sánchez, Polym. Bull., 39 (1997) 465.

33 M. L. Arnal, Z. H. Heránndez, M. Matos, J. J. Sánchez, G. Méndez, A. Sánchez and A. J. Müller, ANTEC Proceed., (1998) 611.

34 J. J. Mara and K. P. Menard, Acta Polymerica, 45 (1994) 387.

35 P. Schouterden, G. Groenicks, B. Van des Heijden and F. Jansen, Polymer, 28 (1987) 2099.

36 D. Parikh, B. S. Childress and G. W. Knight, ANTEC Proceed., (1990) 1543.

37 B. Monrabal, J. Appl. Polym. Sci., 52 (1994) 491.

38 S. A. Karoglanian and I. R. Harrison, Thermochim. Acta, 212 (1992) 143.

39 R. A. Shanks and G. Amarasinghe, unpublished results.

40 L. Woo, S. P. Westphal, T. K. Ling and A. R. Khare, Polym. Preprints, 39 (1998) 203.

41 J. N. Hay and X. Zhou, Polymer, 34 (1993) 1002.

42 M. J. Hill, R. Morgan and P. J. Barham, Polymer, 38 (1997) 3003.

43 K. W. Swogger, G. M. Lancaster, S. Y. Lai and T. I. Butler, J. Plastic Film and Sheeting, 11 (1995) 102.

44 T. I. Butler, S. Y. Lai and R. Patel, J. Plastic Film and Sheeting, 10 (1994) 102.

45 H. Zhou and G. L. Wilkes, Polymer, 38 (1997) 5735.

46 R. A. Shanks and G. Amarasinghe, Polymer, in press.

47 A. J. Müller, M. L. Arnal, G. Méndez and J. J. Sánchez, IUPAC 37th International Symposium on Macromolecules, Gold Coast, Australia, 12–17 July (1998) 85.

48 M. L. Arnal, J. J. Sánchez and A. J. Müller, ANTEC Proceed., (1999) 2329.